



STUDIECENTRUM VOOR KERNENERGIE  
CENTRE D'ÉTUDE DE L'ÉNERGIE NUCLÉAIRE

# THE BRONCHIAL DOSEMETER

S. Oberstedt and H. Vanmarcke

Radioprotection  
SCK•CEN

BLG-667

November 1994

# **THE BRONCHIAL DOSEMETER**

**S. Oberstedt and H. Vanmarcke**

**Radioprotection  
SCK•CEN**

**BLG-667**

**November 1994**

# THE BRONCHIAL DOSEMETER

S. Oberstedt and H. Vanmarcke

Studiecentrum voor Kernenergie SCK•CEN, Boeretang 200, B - 2400 Mol, Belgium

## Abstract

Since some decades it is known, that most of the radiation dose to the lung is due to the inhalation of the short-lived decay products of  $^{222}\text{Rn}$ . Their deposition in the respiratory tract strongly depends on the attachment rate to aerosol-particles present in the indoor air and their plate-out rate to the surfaces. Instead of measuring the activity size distribution of the airborne decay products, knowledge on the respiratory tract retention has been incorporated in the design of a measurement system, called bronchial dosimeter, to assess the lung dose directly. The simulation of the deposition characteristics of the short-lived radon daughters in the nasal cavity and the bronchial tree is based on the comparison of the model of the respiratory tract with results from screen penetration theory. A bronchial dosimeter consisting of three sampling heads has been built and calibrated.

submitted to *Rad. Prot. Dosim.*

## 1. Introduction

During the last decade the radon issue has become one of the major problems in radiation protection. Already 40 years ago it was found, that the lung dose in uranium miners is not due to radon ( $^{222}\text{Rn}$ ) but to the inhalation of its short-lived decay products  $^{218}\text{Po}$ ,  $^{214}\text{Pb}$  and  $^{214}\text{Bi}$ ( $^{214}\text{Po}$ ) [1,2,3]. The airborne decay products of radon deposit in the respiratory tract leading to a radiation dose to the lung. In the indoor environment this deposition strongly depends on the attachment rate of the freshly formed decay products to aerosol-particles and on the plate-out rate to indoor surfaces. Knowledge of the unattached size distribution is important, because the penetration of the nasal cavity increases by one order of magnitude for particles between 1 and 10 nm [4]. The maximum tracheobronchial deposition occurs at about 5 nm [5]. Since it is known that the unattached fraction of the decay products is a major contributor to the radiation dose, several attempts have been made to measure the activity size distribution of the unattached fraction. These measurements on the basis of wire-screen methods were only partially successful, because there are intrinsic problems to separate the unattached fraction completely from the rest of the activity size distribution [6].

Therefore, it has been suggested to simulate the deposition characteristics of the short-lived radon daughters in the nasal and bronchial regions and measure the deposited activity directly. In ref. [7] the theoretical concept of such a measurement system has been presented in detail. According to these specifications a so-called bronchial dosimeter has been built at the Belgian Nuclear Research Center, SCK•CEN. In the following the design and the efficiency determination of this bronchial dosimeter will be reported.

## 2. Description of the bronchial dosimeter

Basically, it is assumed that the deposition characteristics of the nasal cavity and the bronchial tree may be simulated by different numbers of screens [8,9]. Their respective sizes and numbers are determined by comparing models of the respiratory tract with results from the screen penetration theory. From recent investigations on the relationship between nasal deposition, inspiratory flow rate and the particle diffusion coefficient [10] it follows that, for an average nasal inspiration flow rate of 30 l/min, a 400 mesh screen operated at a face velocity of about 12 cm/s provides a rather good approximation to the nasal absorption characteristics. Adding

up four such screens provides a good approximation to the bronchial tree [11,12].

The bronchial dosimeter consists basically of two different units. The first unit is the sampling section, which is used to collect the airborne radon decay products. This part of the dosimeter consists of three different sampling channels :

1. The sampling head of the first channel consists of an open-faced polycarbonate membrane filter with a pore size of  $0.4 \mu\text{m}$ , which collects the total airborne activity.
2. In the second head the filter is covered by a 400 mesh screen in order to collect the activity penetrating the nasal cavity. The activity deposited in the nasal cavity is then given by the difference between the activity collected on filter (1) and filter (2).
3. The filter of the third sampling head is covered by five 400 mesh screens to collect the difference between the airborne activity and what deposits in the nasal cavity plus bronchial tree. From the difference between the activity collected on filters (2) and (3) the activity absorbed in the bronchial tree is obtained.

The sampling section of the bronchial dosimeter is shown in Fig. 1. Each sampling channel has an open diameter of 4 cm. Therefore, the nominal flow rate  $f_0$  for each channel at normal pressure  $p_0 = 1.013 \times 10^5 \text{ Pa}$  and at a temperature  $T_0 = 293 \text{ K}$  has been adjusted to be 9.1 l/min in order to get the required face velocity of 12 cm/s. Since the flow rate changes with  $p$  and  $T$ , the corrected flow rate  $f_c$  has to be considered :

$$f_c = f_0 \sqrt{p/p_0 T_0/T} \quad (1)$$

In order to minimize fluctuations in the sampling efficiencies the flow rate through each channel is stabilized by a limiting orifice.

The second unit of the bronchial dosimeter is the alpha-spectrometer section which consists of three separate  $\alpha$ - detectors. After sampling the filters remain mounted on their sampling heads in order to keep the counting geometry reproducible. The sampling heads are put into the vacuum chambers, where the filter activities due to the  $\alpha$ - decay of  $^{218}\text{Po}$  and  $^{214}\text{Po}$  are measured. From the peak areas obtained in three subsequent measurements the decay product concentrations of  $^{218}\text{Po}$ ,  $^{214}\text{Pb}$ ,  $^{214}\text{Bi}$  and  $^{214}\text{Po}$  collected on the filters can be calculated. The  $\alpha$ - particles are measured using  $900 \text{ mm}^2$  passivated implanted planar silicon (PIPS) detectors. The distance between filter and detector is about 0.7 cm, and the vacuum chamber is operated at a pressure of  $10^4 \text{ Pa}$ . The energy resolution of each detector is better than

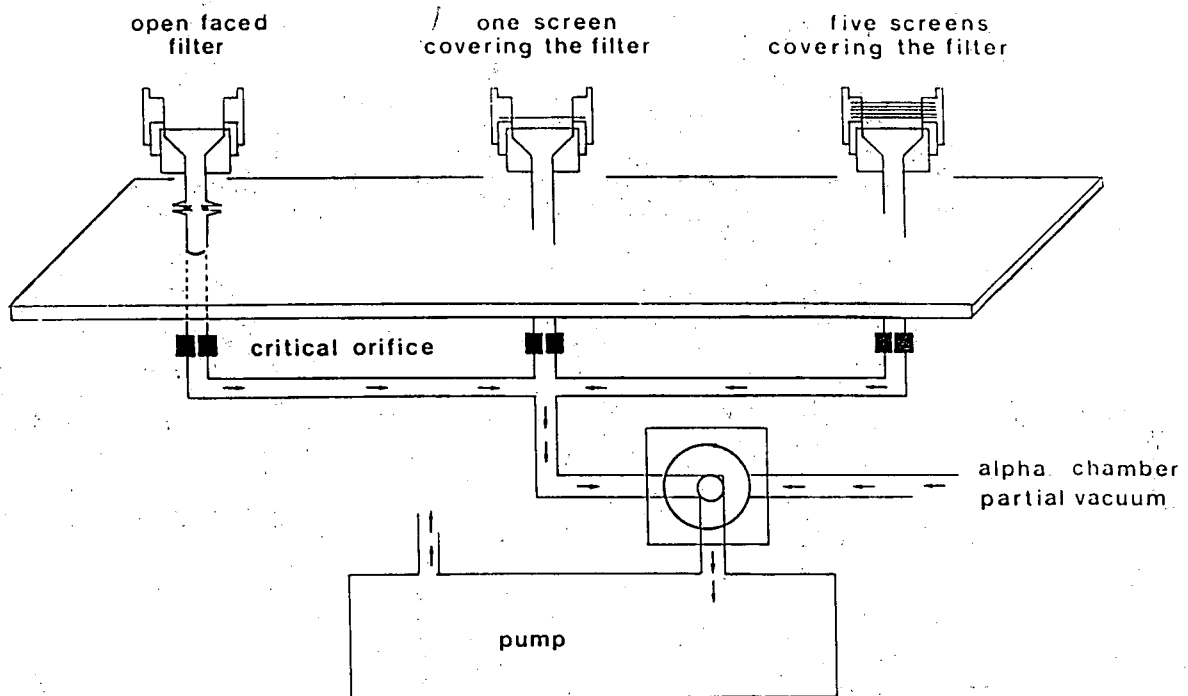


Fig. 1: Sampling section of the bronchial dosimeter. The open diameter of one sampling channel is 4 cm. The flow rate at standard atmospheric conditions is 9.1 l/min leading to a face velocity of 12 cm/s.

30 keV at an  $\alpha$ -particle energy of about 5.5 MeV. The energy calibration was performed with a mixed source containing  $^{239}\text{Pu}$ ,  $^{241}\text{Am}$  and  $^{244}\text{Cm}$  with  $\alpha$ -particle energies at 5.16 MeV, 5.49 MeV and 5.81 MeV, respectively.

### 3. Efficiency determination

The efficiency of the bronchial dosimeter is determined by the efficiency of one sampling channel and the intercomparison of all three channels. The efficiency of one sampling channel is determined by measuring the  $\alpha$ -activity from  $^{218}\text{Po}$  and  $^{214}\text{Po}$  and the  $\gamma$ -activity following the  $\beta$ -decay of  $^{214}\text{Bi}$ .

First, the efficiency of the germanium detector has been determined for the respective filter

**Table 1:** Efficiencies of the three sampling channels of the bronchial dosimeter. The indicated uncertainties denote one weighted standard deviation of the mean.

	head(1)	head(2)	head(3)
efficiency $\epsilon_\alpha$	$0.1492 \pm 0.0016$	$0.1620 \pm 0.0017$	$0.1517 \pm 0.0010$

geometry with four  $^{134}\text{Cs}$  sources. This isotope provides a  $\gamma$ - line at  $E_\gamma = 604.7$  keV which is close to that in  $^{214}\text{Bi}$  ( $E_\gamma = 609.3$  keV). The  $^{134}\text{Cs}$ -activity was distributed homogeneously over a disk with the same area as the active part of the filter. The cascade summing corrections for a distance between filter and detector of 3.75 cm were derived from refs. [13,14]. The photon branching ratio for the caesium peak being 0.976 and 0.448 for the bismuth peak were taken from ref. [15]. The detection efficiency of the germanium detector at  $E_\gamma = 609.3$  keV was

$$\epsilon_{Ge}(609.3\text{keV}) = (9.74 \pm 0.20) \times 10^{-3} \quad (2)$$

During the efficiency determination the sampling section of the bronchial dosimeter was placed in a chamber with a volume of about  $6 \text{ m}^3$ . The radon activity concentration  $c_{Rn}$  varied between  $26 \text{ kBq/m}^3$  and  $10 \text{ kBq/m}^3$ . The sampling time was chosen to be 10 min.

After sampling the filters were transferred to the vacuum chambers within 1 min. The  $\alpha$ - activity of all sampling heads were measured for 5 min and then for 15 min. Afterwards, the sampling head of channel (1) was transferred to the germanium detector. The  $\gamma$ - activity of filter (1) and the  $\alpha$ - activities of filter (2) and (3) were measured for 30 min. From the area under the  $\gamma$ - peak at  $E_\gamma = 609.3$  keV, the photon branching ratio and  $\epsilon_{Ge}$  the expected number of  $\alpha$ - particles  $N_\alpha^{(e)}$  from  $^{214}\text{Po}$  is determined. The detection efficiency for  $\alpha$ - particles  $\epsilon_\alpha$  of this sampling channel is then the ratio between the number of  $\alpha$ - particles extrapolated from the  $\alpha$ - measurements,  $N_\alpha^{(m)}$ , and  $N_\alpha^{(e)}$ .

From six measurements the efficiency of sampling channel (1) was obtained to be

$$\epsilon_{\alpha,1} = 0.1492 \pm 0.0041 \quad (3)$$

at one standard deviation. The respective data are shown in Fig. 2. From these data the efficiency of the other two sampling channels were determined by intercomparing the equilibrium

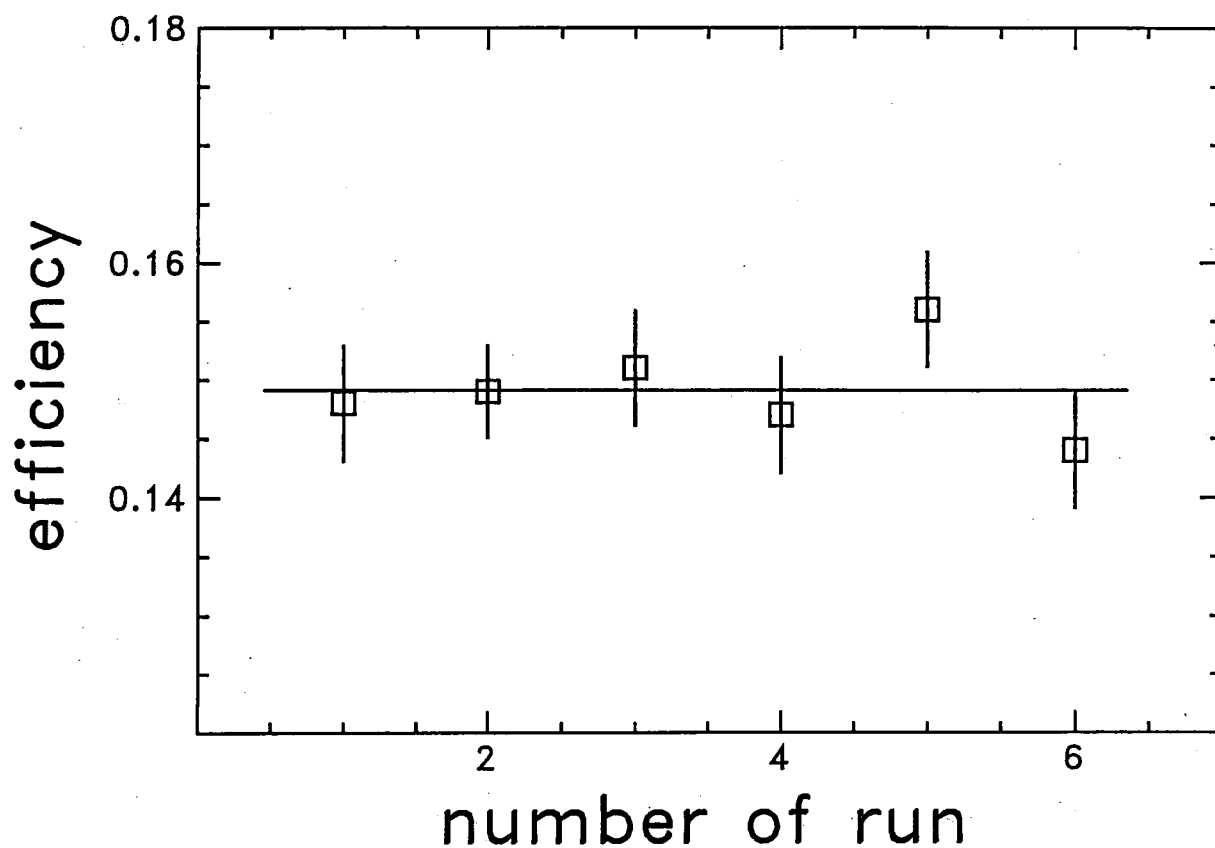


Fig. 2: Efficiency of sampling channel (1) obtained at a distance of 0.7 cm from the detector. The full line indicates the weighted average of the data.

equivalent radon concentrations (EEC). The EEC of a non-equilibrium mixture of short-lived radon daughters in air is the activity concentration of radon in radioactive equilibrium with its daughters, which have the same potential alpha energy concentration as the actual non-equilibrium mixture (for details see e. g. ref. [16]). The obtained sampling efficiencies are given in Tab. 1. Their relative uncertainty on the mean value is less than 1.1 % at one standard deviation.

#### 4. First experimental experience

Under laboratory conditions test measurements with the complete system were performed. In the beginning the radon concentration was about 4.5 kBq/m<sup>3</sup> and drops to about 1.5 kBq/m<sup>3</sup> at the end of the test period. The sampling period was 5, 6 or 7 min. The filter activities

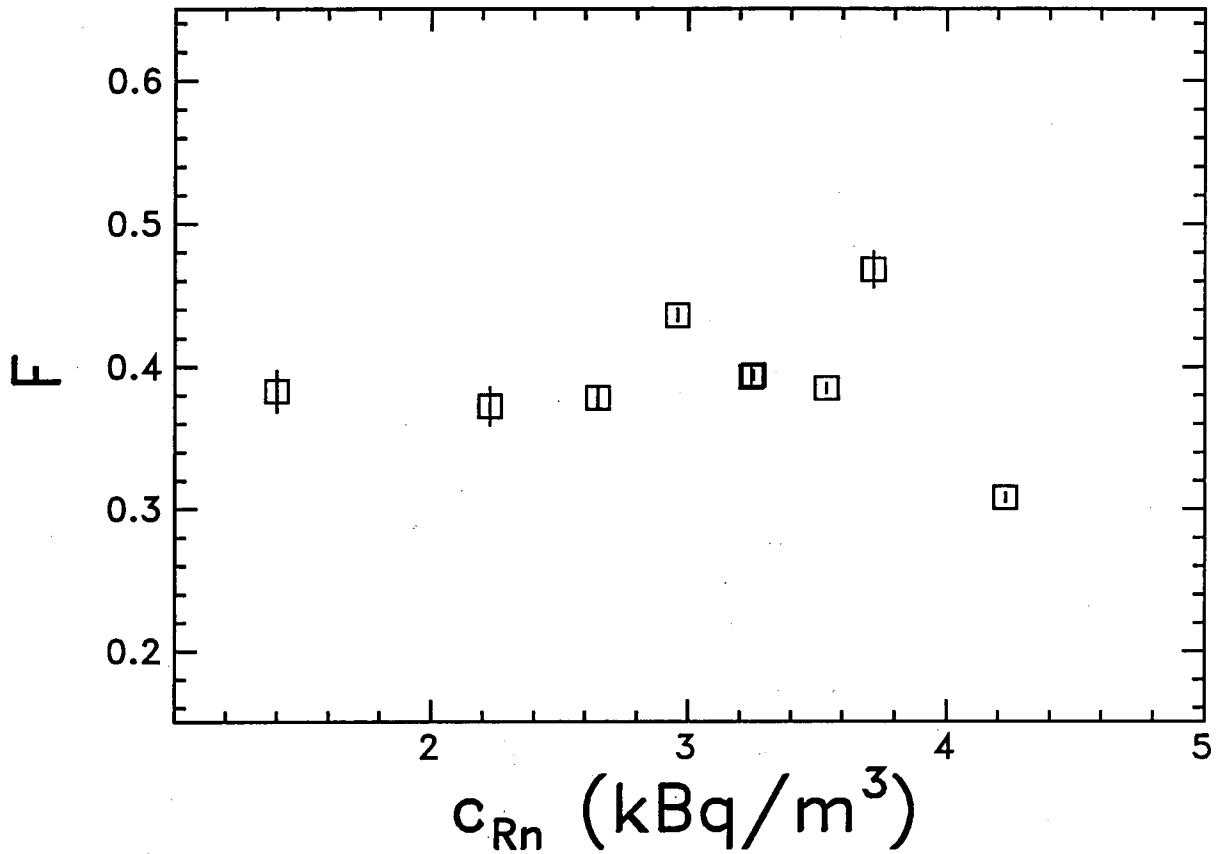


Fig. 3: Equilibrium factor  $F$  as a function of the radon concentration  $c_{Rn}$ . The average value for  $F = 0.39$  with a relative standard deviation less than 11 %.

were measured during two periods for 10 min and 35 min, respectively.

From the open-faced filter of sampling channel (1) the EEC in air was obtained. Division of an EEC-value by its corresponding radon activity concentration  $c_{Rn}$  gives the equilibrium factor  $F$ , which characterizes the disequilibrium between the daughter mixture and radon (for details on that definition see e. g. ref. [16]). Since the daughter mixture strongly depends on the competition between the attachment rate and the plate-out rate to the indoor surfaces,  $F$  also gives a characterization of the aerosol-concentration present. In Fig. 3  $F$  is shown as a function of  $c_{Rn}$ . The data show that the atmospheric conditions were rather stable throughout the measurement campaign. The average equilibrium factor throughout the test measurements was 0.39 with a relative uncertainty less than 11 % at one standard deviation. The obtained fractional deposition of the short-lived decay products in the nasal cavity ( $f_n$ )

**Table 2:** Average fractional deposition of the short-lived radon decay products in the nasal cavity  $\bar{f}_n$  and the bronchial tree  $\bar{f}_b$ . The values are averaged over nine measurements with equilibrium factors  $F = 0.39 \pm 0.04$ .

average fractional deposition	$^{218}\text{Po}$ $10^{-2}$	$^{214}\text{Pb}$ $10^{-2}$	$^{214}\text{Bi}$ $10^{-2}$	EEC $10^{-2}$
nasal cavity $\bar{f}_n$	$1.3 \pm 1.3$	$-0.3 \pm 2.2$	$0.5 \pm 1.9$	$0.4 \pm 0.7$
bronchial tree $\bar{f}_b$	$4.4 \pm 1.0$	$1.1 \pm 1.6$	$2.5 \pm 2.0$	$1.9 \pm 0.5$

as well as in the bronchial tree ( $f_b$ ) is shown as a function of  $F$  in Fig. 4 for each nuclei separately. Although the data show some fluctuations, it is still valid to define average fractional depositions for the different decay products. Average values  $\bar{f}_n$  and  $\bar{f}_b$  taken from the data of ten measurements are summarized in Tab. 2.

## 6. Conclusion

According the conceptual design of a multiple wire screen sampler in ref. [7] a bronchial dosimeter has been built. The efficiency determination was completed and first test measurements were performed under laboratory conditions. From these measurements it turned out, that the bronchial dosimeter is a suitable facility to individually survey deposition characteristics of the different short-lived radon decay products in the nasal cavity as well as in the bronchial tree. Further investigations should be concerned with the fractional depositions as a function of the aerosol concentration, i. e. their dependence on the equilibrium factor  $F$ . However, it has always to be taken into account that the interpretation of the data strongly depend on the underlying model of the respiratory tract, which influences the choice of the mesh size as well as the number of screens used for the sampling heads. For instance, according recent model calculations [18] the nasal absorption might be better simulated by a screen with a 100 mesh grid.

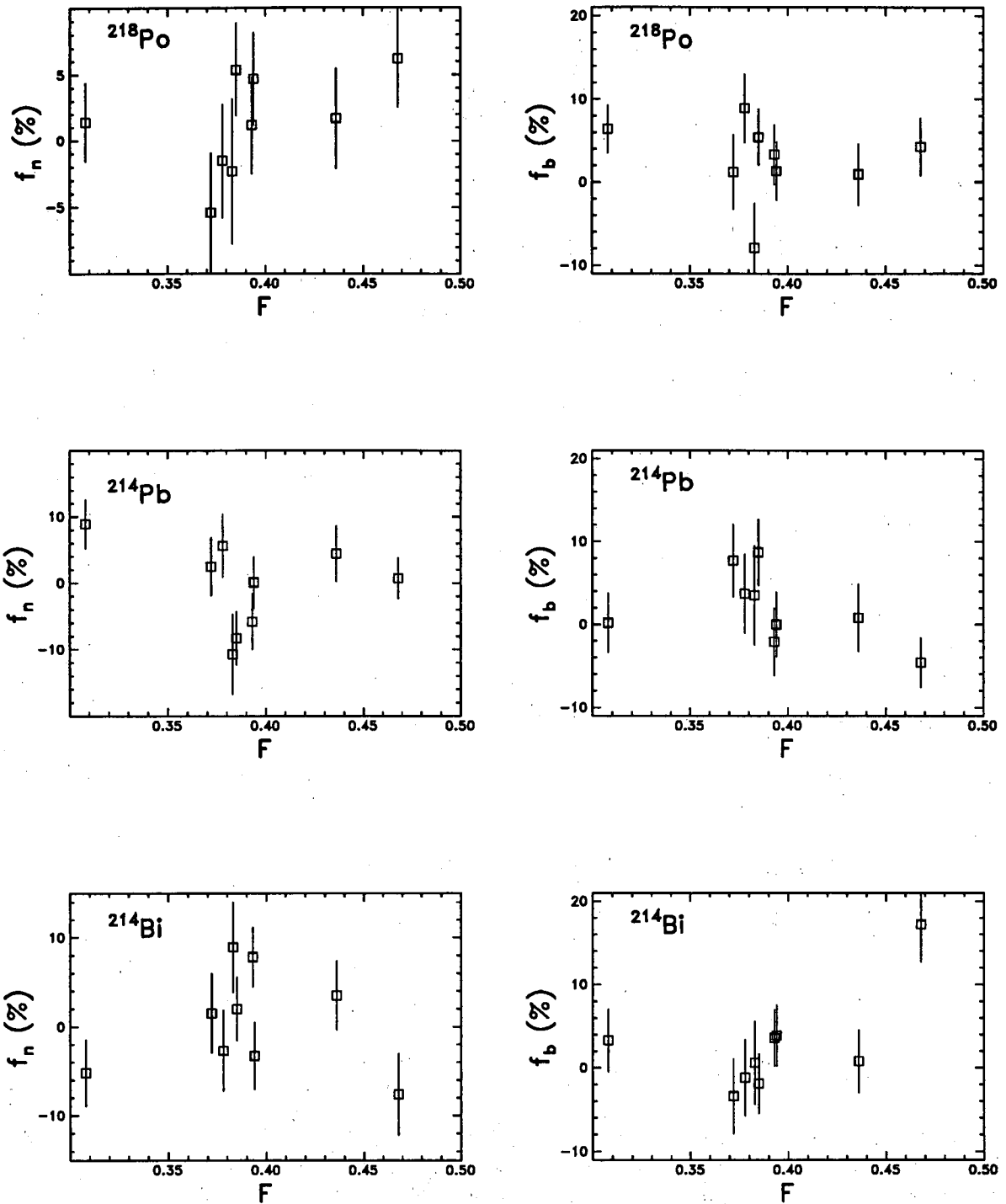
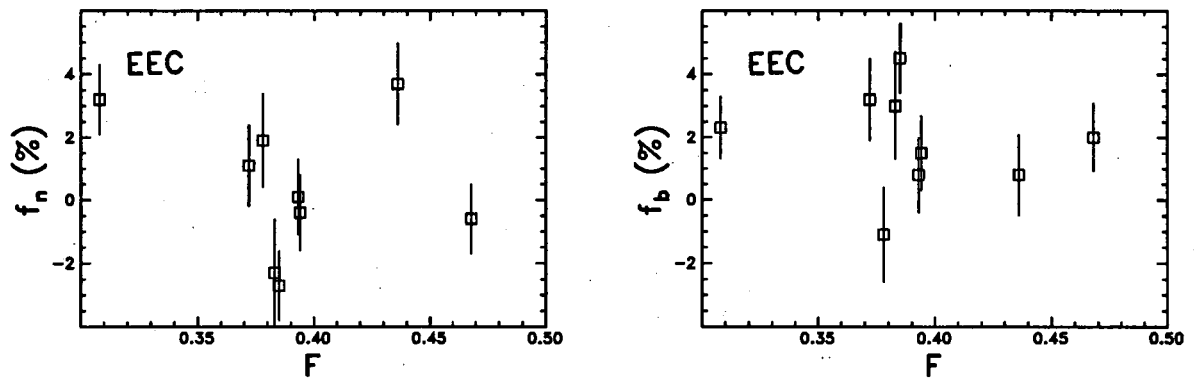


Fig. 4: Fractional deposition of the short-lived radon decay products  $^{218}\text{Po}$ ,  $^{214}\text{Pb}$  and  $^{214}\text{Bi}$  as a function of the equilibrium factor  $F$ . The left part shows the fraction of decay products deposited in the nasal cavity ( $f_n$ ), and the right part shows the fractional deposition in the bronchial tree ( $f_b$ ).



**Fig. 5:** Fractional equilibrium equivalent radon concentration (EEC) as a function of the equilibrium factor  $F$ . The left part shows the fraction deposited in the nasal cavity ( $f_n$ ), and the right part shows the fractional deposition in the bronchial tree ( $f_b$ ).

This work was supported by the Commission of the European Communities .

## References

- [1] Shapiro J., Univ. of Rochester Rep. UR-298 (1954)
- [2] Aurand P., W. Jacobi and A. Schraub, Sonderband für Strahlentherapie 35 (1955) 237
- [3] Bale W. F. and J. V. Shapiro, Proceedings of the First International Conference on Peaceful Use of Atomic Energy, Geneva Vol. 13 (1955), 233, United Nations (1956)
- [4] Swift D. L., N. Montassier, P. K. Hopke, K. Karpen-Hayes, Y. S. Cheng, Y. F. Su, H. C. Yeh and J. C. Strong, J. Aerosol Sci. 23 (1992) 65
- [5] Hopke P. K., Health Physics 63 (1992) 209

- [6] Ramamurthi, M. and P. H. Hopke, Health Physics 56 (1989) 189
- [7] Hopke P. H., M. Ramamurthi and E. O. Knudson, Health Physics 58 (1990) 291
- [8] Cheng Y. S. and H. C. Yeh, J. Aerosol Sci. 11 (1980) 313
- [9] Cheng Y. S., J. A. Keating and G. M. Kanapilly, J. Aerosol Sci. 11 (1980) 549
- [10] Cheng Y. S., Y. Yamamda, H. C. Yeh and D. L. Swift, J. Aerosol Sci. 19 (1988) 741
- [11] James A. C., Radon and its Decay Products (edited by P. K. Hopke) ACS Symposium Series 331 (1987), 400
- [12] James A. C., Radon and its Decay Products in Indoor Air (edited by W. W. Nazaroff and A. V. Nero) Wiley-Interscience (1988) 259
- [13] Schirma F. J. and D. D. Hoppes, Appl. Rad. Isot. 34 (1983) 1109
- [14] Griffiths R., Nucl. Instr. Meth. 91 (1971) 377
- [15] Browne E., J. M. Dairiki and R. E. Doebler, Table of Isotopes (edited by C. M. Lederer and V. S. Shirley) seventh edition (1978) 1367
- [16] Porstendörfer J., Fifth International Symposium on the Natural Radiation Environment (tutorial sessions), edited by the Commission of the European Communities, EUR 14411 EN (1993) 69
- [17] Wilkening M., Studies in Environmental Science 40 (Radon in the Environment), Elsevier (1990) 126
- [18] George A. C. and E. O. Knutson, Radiat. Prot. Dosim. 45 (1992) 689